JACS
JOURNAL OF THE AMERICAN CHEMICAL SOCIETY

Subscriber access provided by ISTANBUL TEKNIK UNIV

Article

Theoretical Study of the Mechanism of Hantzsch Ester Hydrogenation of Imines Catalyzed by Chiral BINOL-Phosphoric Acids

Luis Simo#n, and Jonathan M. Goodman

J. Am. Chem. Soc., **2008**, 130 (27), 8741-8747 • DOI: 10.1021/ja800793t • Publication Date (Web): 11 June 2008

Downloaded from http://pubs.acs.org on February 8, 2009

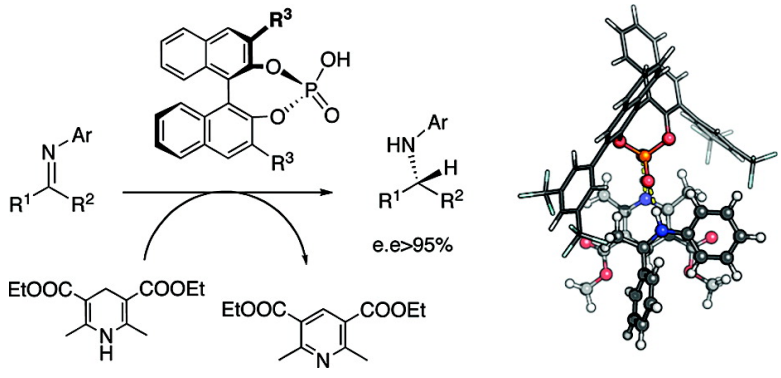

More About This Article

Additional resources and features associated with this article are available within the HTML version:

- Supporting Information
- Links to the 3 articles that cite this article, as of the time of this article download
- Access to high resolution figures
- Links to articles and content related to this article
- Copyright permission to reproduce figures and/or text from this article

View the Full Text HTML

ACS Publications
High quality. High impact.

Journal of the American Chemical Society is published by the American Chemical Society. 1155 Sixteenth Street N.W., Washington, DC 20036

J|A|C|S
ARTICLES

Published on Web 06/11/2008

Theoretical Study of the Mechanism of Hantzsch Ester Hydrogenation of Imines Catalyzed by Chiral BINOL-Phosphoric Acids

Luis Simón and Jonathan M. Goodman*

Unilever Centre For Molecular Science Informatics, Department of Chemistry, Lensfield Road, Cambridge CB2 1EW, U.K.

Received January 31, 2008; E-mail: J.M.Goodman@ch.cam.ac.uk

Abstract: The mechanism of the Hantzsch ester hydrogenation of imines catalyzed by chiral BINOL-phosphoric acid has been investigated using DFT methods. Despite the importance of this reaction, there are a number of possible detailed mechanisms, and the preferred pathway has not been firmly established. Our calculations show that the catalyst not only activates the imine group for the reaction by acting as a Brønsted acid but also establishes an interaction with the Hantzsch ester that can lead to an explanation for the enantioselectivity.

Introduction

The hydrogenation of imines using Hantzsch esters (Scheme 1) can be catalyzed by Brønsted acids, including chlorosulfonic, trifluoroacetic and diphenylphosphoric acids.[1–3] This reaction has received recent interest.[4,5] Chiral BINOL-phosphoric acid derivatives[6] with bulky substituents have been found to show high degrees of enantioselectivity in this reaction.[7–17]These catalysts have also been employed successfully in enantioselective Strecker,[18,19] Mannich,[20–23] hetero-Diels−Alder,[24] Friedel−Craft,[25–29] aza-ene-type,[30,31] acylcyanation,[32] conjugated additions,[33] and Pictet−Spengler[34] reactions.

Scheme 1. Hantzsch Ester Hydride Transfer Reaction and Structure of the Catalysts

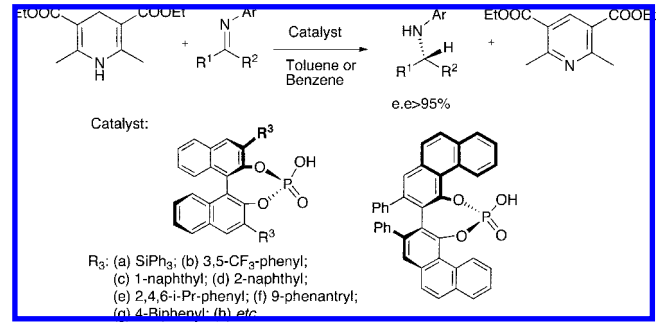

Structures derived from X-ray diffraction experiments of crystals of the Brønsted acid[7,9,10] and of the imine−Brønsted acid complex[11] have been used to explain the enantioselectivity of this reaction (Figure 1, Mechanism A). According to this model, the Hantzsch ester approach should be preferred on one face of the imine. Since the imine interacts with the catalyst by a single H-bond, its orientation with respect to the catalyst is not fixed. Conformations leading to opposite enantiomers may be expected to have only small energy differences. An alternative mechanism, in which the phosphate catalyst establishes H-bonds with both nucleophile and imine group has been proposed for BINOL-phosphoric acid-catalyzed Mannich,[21] aza-

(1) Rueping, M.; Azap, C.; Sugiono, E.; Theissmann, T. *Synlett* **2005**, 2367–2369.
(2) Rueping, M.; Theissmann, T.; Antonchick, A. P. *Synlett* **2006**, 1071–1074.
(3) Itoh, T.; Nagata, K.; Miyazaki, M.; Ishikawa, H.; Kurihara, A.; Ohsawa, A. *Tetrahedron* **2004**, *60*, 6649–6655.
(4) Connon, S. J. *Org. Biomed. Chem.* **2007**, *5*, 3407–3417.
(5) You, S.-L. *Chem.—Asian J.* **2007**, *2*, 820–827.
(6) Akiyama, T. *Chem. Rev.* **2007**, *107*, 5744–5758.
(7) Rueping, M.; Sugiono, E.; Azap, C.; Theissmann, T.; Bolte, M. *Org. Lett.* **2005**, *7*, 3781–3783.
(8) Hoffmann, S.; Nicoletti, M.; List, B. *J. Am. Chem. Soc.* **2006**, *128*, 13074–13075.
(9) Rueping, M.; Antonchick, A. P.; Theissmann, T. *Angew. Chem., Int. Ed.* **2006**, *45*, 3683–3686.
(10) Rueping, M.; Antonchick, A. P.; Theissmann, T. *Angew. Chem., Int. Ed.* **2006**, *45*, 6751–6755.
(11) Storer, R. I.; Carrera, D. E.; Ni, Y.; MacMillan, D. W. C. *J. Am. Chem. Soc.* **2006**, *128*, 84–86.
(12) Yang, J. W.; List, B. *Org. Lett.* **2006**, *8*, 5653–5655.
(13) Li, G.; Liang, Y.; Antilla, J. C. *J. Am. Chem. Soc.* **2007**, *129*, 5830–5831.
(14) Zhou, J.; List, B. *J. Am. Chem. Soc.* **2007**, *129*, 7498–7499.
(15) Hoffmann, S.; Seayad, A. M.; List, B. *Angew. Chem., Int. Ed.* **2005**, *44*, 7424–7427.
(16) Rueping, M.; Antonchick, A. P. *Angew. Chem., Int. Ed.* **2007**, *46*, 4562–4565.
(17) Guo, Q.-S.; Du, D.-M.; Xu, J. *Angew. Chem., Int. Ed.* **2008**, *47*, 759–762.
(18) Rueping, M.; Sugiono, E.; Azap, C. *Angew. Chem., Int. Ed.* **2006**, *45*, 2617–2619.
(19) Rueping, M.; Sugiono, E.; Moreth, S. A. *Adv. Synth. Catal.* **2007**, *349*, 759–764.
(20) Yamanaka, M.; Itoh, J.; Fuchibe, K.; Akiyama, T. *J. Am. Chem. Soc.* **2007**, *129*, 6756–6764.
(21) Guo, Q.-X.; Liu, H.; Guo, C.; Luo, S.-W.; Gu, Y.; Gong, L.-Z. *J. Am. Chem. Soc.* **2007**, *129*, 3790–3791.
(22) Uraguchi, D.; Terada, M. *J. Am. Chem. Soc.* **2004**, *126*, 5356–5357.
(23) Akiyama, T.; Itoh, J.; Yokota, K.; Fuchibe, K. *Angew. Chem., Int. Ed.* **2004**, *43*, 1566–1568.
(24) Liu, H.; Cun, L.-F.; Mi, A.-Q.; Jiang, Y.-Z.; Gong, L.-Z. *Org. Lett.* **2006**, *8*, 6023–6026.
(25) Qiang Kang, Q.; Zhao, Z.-A.; You, S.-L. *J. Am. Chem. Soc.* **2007**, *129*, 1484–1485.
(26) Jia, Y.-X.; Zhong, J.; Zhu, S.-F.; Zhang, C.-M.; Zhou, Q.-L. *Angew. Chem., Int. Ed.* **2007**, *46*, 5565–5567.

 © 2008 American Chemical Society

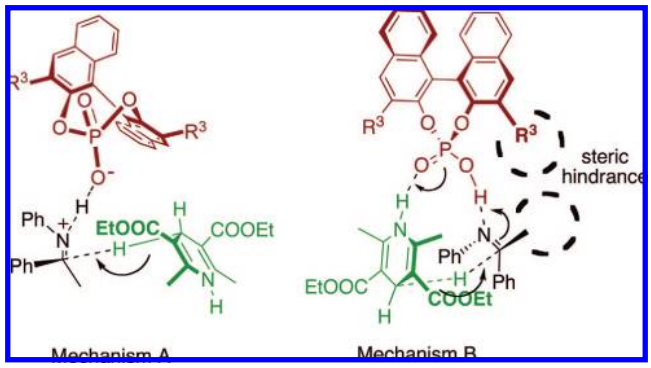

Figure 1. Possible mechanisms for the Hantzsch ester hydrogenation of imines.

ene type,[30] Friedel−Craft,[26] hydrophosphonylation[35] and Nazarov reactions[36] (Figure 1, Mechanism B). To the best of our knowledge, this mechanism (Mechanism B) has not been proposed for the hydrogenation reaction, nor has a theoretical study has been performed on reactions catalyzed by BINOL-phosphoric acid derivative catalyst. The only previous computational study deals with the Mannich addition of silyl ethers,[20] where a process similar to Mechanism B is not possible because of the absence of a suitable hydrogen in the nucleophile.

Mechanism B explains the high enantioselectivity using the "three point interaction model".[37] According to this model, in order to observe chiral recognition or enantioselectivity, there must exist at least three interactions between the host and the guest or between the catalysts and the transition state, and at least one of these interactions must be stabilizing. Mechanism B shows two H-bonds between the catalyst and reactants in the transition state. The third interaction is a consequence of steric contacts between the transition state and bulky groups in the catalyst. It is possible that both *Z*- and *E*-imines might react through this transition state, and the three controlling interactions suggest that a change from an *E*- to a *Z*-imine conformation should lead to the opposite enantiomer of the product amine.

In this paper, we use DFT calculations to study the mechanism of this reaction, investigating both the effects of the three-point binding model and the stereochemical consequences of *E*-/*Z*-imine isomerization.

Computational Methods

From the substrates reported in the literature,[7,9–11,13,14] we selected the imine of acetophenone as a representative example (R^1 = Me, R^2 = Ph). Although in most experiments *N*-paramethoxyphenyl imines were studied (Ar = PMP), similar enantioselectivities and yields were obtained for *N*-phenyl imines (R^3 = Ph),[11] and thus these simpler molecules have been used in the calculations. The dimethyl Hantzsch ester was used instead of the diethyl ester, and the BINOL group was replaced by buta-1,3-diene-1,4-diol-phosphoric acid for the first studies.

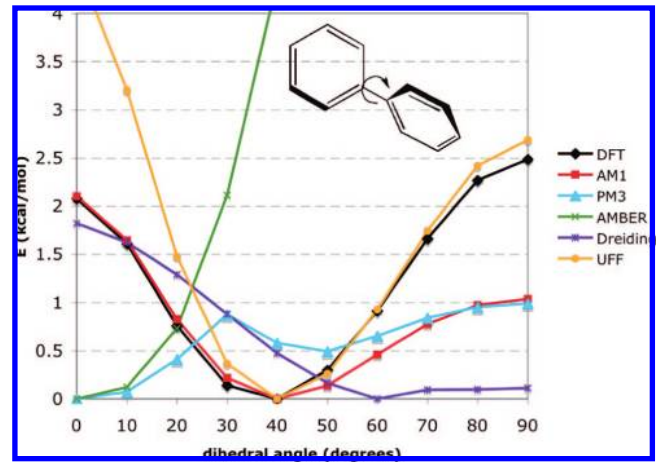

Figure 2. Performance of different semiempirical and force fields in reproducing energies for different dihedral angles on biphenyls.

Using these simplified models, transition-state structures were located using the Jaguar[38] program. Calculations were done in the gas phase with B3LYP[39] functional and 6-31+G*[40–42] basis set, augmented with polarization and diffuse functions for hydrogens which are transferred or bonded to heteroatoms. Vibrational contributions to Gibbs free energy were calculated at this level of theory. For each optimized structure, the single-point energy was calculated (B3LYP/6-31++G**) with solvent (toluene) included implicitly using a self-consistent reaction-field method as implemented in Jaguar. This energy was added to the Gibbs energy correction calculated previously. Energy barriers are relative to the corresponding starting materials, in all cases.

Although different conformations of the model catalyst have been investigated, corresponding to different enantiomers in the real catalysts, only very small energy differences were observed. The lowest-energy structures are included in the discussion.

NBO[43] analysis was done on the resulting wave function using NBO 5.0 included in Jaguar. The bonding pattern that was used for the NBO calculations on the transition structures is shown in Figure 1, mechanism B.

Calculations on complete catalysts were performed using ONIOM[44–46] methodology as implemented in the Gaussian03[47] program. The high-level layer was treated using B3LYP/6-31G*[40–42] level of theory (the basis set was augmented with polarization functions for the transferable hydrogen atoms and for those bonded

(27) Li, G.; Rowland, G. B.; Rowland, E. B.; Antilla, J. C. *Org. Lett.* **2007**, *9*, 4065–4068.
(28) Terada, M.; Sorimachi, K. *J. Am. Chem. Soc.* **2007**, *129*, 292–293.
(29) Terada, M.; Yokoyama, S.; Sorimachi, K.; Uraguchi, D. *Adv. Synth. Catal.* **2007**, *349*, 1863–1867.
(30) Terada, M.; Machioka, K.; Sorimachi, K. *Angew. Chem., Int. Ed.* **2006**, *45*, 2254–2257.
(31) Terada, M.; Machioka, K.; Sorimachi, K. *J. Am. Chem. Soc.* **2007**, *129*, 10336–10337.
(32) Pan, S. C.; Zhou, J.; List, B. *Angew. Chem., Int. Ed.* **2007**, *46*, 612–614.
(33) Jiang, J.; Yu, J.; Sun, X.-X.; Rao, Q.-Q.; Gong, L.-Z. *Angew. Chem., Int. Ed.* **2008**, *47*, 2458–2462.
(34) Wanner, M. J.; van der Haas, R. N. S.; de Cuba, K. R.; van Maarseveen, J. H.; Hiemstra, H. *Angew. Chem., Int. Ed.* **2007**, *46*, 7485–7487.
(35) Akiyama, T.; Morita, H.; Itoh, J.; Fuchibe, K. *Org. Lett.* **2005**, *7*, 2583–2585.
(36) Rueping, M.; Ieawsuwan, W.; Antonchick, A. P.; Nachtsheim, B. J. *Angew. Chem., Int. Ed.* **2007**, *46*, 2097–2100.
(37) Easson, L. H.; Stedman, E. *J. Biochem.* **1933**, *27*, 1257–1266.
(38) *Jaguar*, version 6.5; Schrödinger Inc.: New York, NY, 2006.
(39) Becke, A. D. *J. Chem. Phys.* **1983**, *98*, 5648–5652.
(40) Gill, P. M. W.; Johnson, B. G.; Pople, J. A.; Frisch, M. J. *J. Chem. Phys.* **1992**, *197*, 499–505.
(41) Krishnam, R.; Binkley, J. S.; Seeger, R.; Pople, J. A. *J. Chem. Phys.* **1980**, *72*, 650–654.
(42) Clark, T.; Chandrasekhar, J.; Schleyer, P. v. R. *J. Comput. Chem.* **1983**, *4*, 294–301.
(43) Glendening, E. D.; Weinhold, F. *J. Comput. Chem.* **1998**, *19*, 593–609.
(44) Dapprich, S.; Komaromi, I.; Byun, K. S.; Morokuma, K.; Frisch, M. J. *J. Mol. Struct. (THEOCHEM)* **1999**, 461–462.
(45) Svensson, M.; Humbel, S.; Morokuma, K. *J. Chem. Phys.* **1996**, *105*, 3654–3661.
(46) Vreven, T.; Morokuma, K. *J. Comput. Chem.* **2000**, *21*, 1419–1432.
(47) Frisch, M. J.; *Gaussian 03*, revision D.03; Gaussian, Inc.: Wallingford CT, 2004.

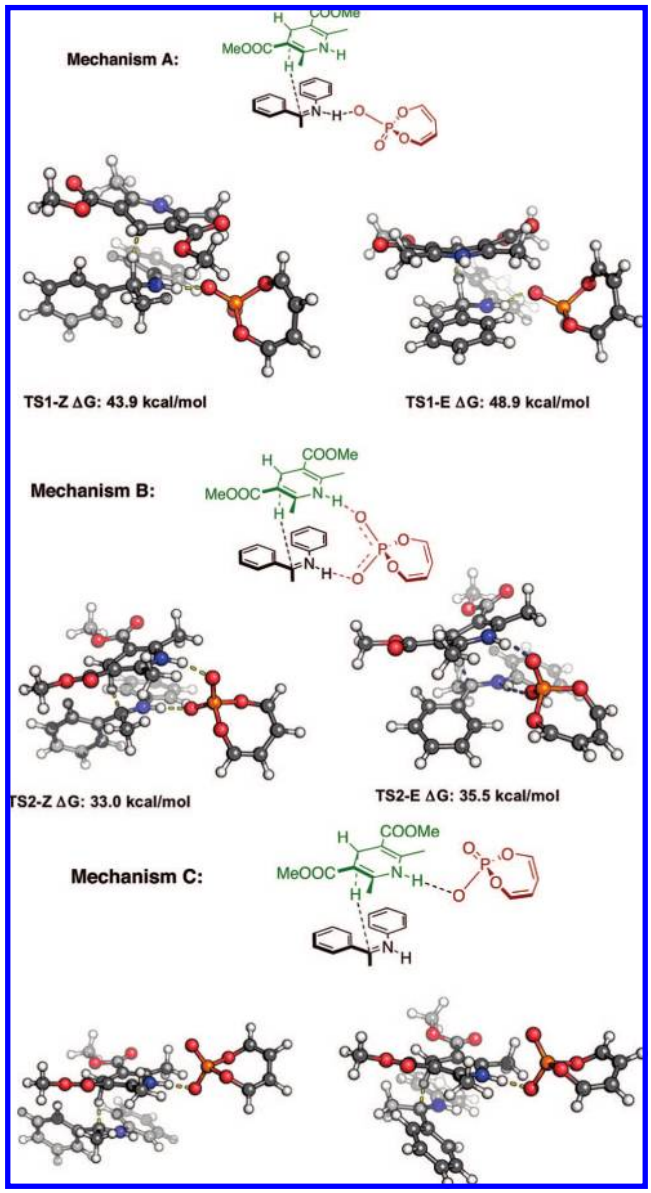

Figure 3. Lowest-energy transition states for the model reaction. A full list is available in the Supporting Information.

to heteroatoms). In Figures 5 and 6, atoms treated with a high level of theory are represented as ball and stick models, while remaining atoms are shown as a wire model.

The method in the low level ONIOM layer should be chosen to reproduce the B3LYP/6-31G* geometry in the region of the catalyst. Although all available semiempirical and molecular mechanics methods are adequate to obtain the right angles and bond distances for aromatic rings, the correct description of dihedral angles between aromatic rings joined by single bonds is more demanding. To test which method describes more correctly this geometrical feature, semiempirical methods (AM1[48] and PM3[49]) and molecular mechanics force fields implemented in Gaussian03 (AMBER,[50] Dreiding,[51] and UFF[52]) were tested on biphenyl. Relaxed scans of

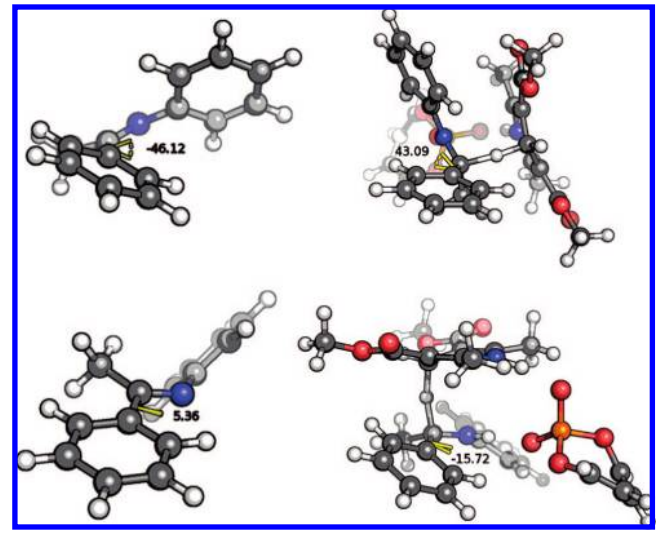

Figure 4. Phenyl dihedrals angles in imines and transition states for *Z* (above) and *E* (below) conformations.

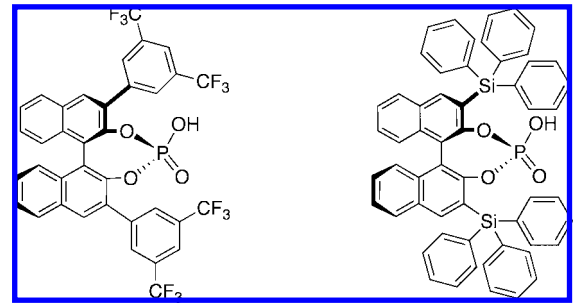

Figure 5. Rueping (left) and MacMillan (right) catalysts.

the dihedral angle on this molecule were performed, and relative energies were compared to that obtained with B3LYP/6-31G* as shown in Figure 2. Only AM1 and UFF come reasonably close to the results obtained for the DFT method. While AM1 fits better for low dihedral angles, UFF reproduces energy values more closely for dihedrals over 40°. We expected that most biphenyl groups will have these higher values, and, therefore, the UFF method was chosen for the low level region.

Once an optimized transition structure was obtained with the ONIOM method, single-point calculations were evaluated using MPWB1K/6-31G** level of theory. This functional was chosen as it has been shown to give good results in describing weak nonbonded (dispersive) interactions.[53] Ultrafine grid and very tight SCF convergence criteria were used in this calculation. Solvent (toluene) effects were included in this single-point energy evaluation by means of the PCM[54–58] solvation model. The cavity for this PCM calculation was defined according to the UAKS[59] scheme.

(48) Dewar, M. J. S.; Reynolds, C. H. *J. Comput. Chem.* **1986**, *2*, 140–143.
(49) Stewart, J. J. P. *J. Comput. Chem.* **1989**, *10*, 221–264.
(50) Cornell, W. D.; Cieplak, P.; Bayly, C. I.; Gould, I. R., Jr.; Ferguson, D. M.; Spellmeyer, D. C.; Fox, T.; Caldwell, J. W.; Kollman, P. A. *J. Am. Chem. Soc.* **1995**, *117*, 5179–5179.
(51) Mayo, S. L.; Olafson, B. D.; Goddard, W. A., III. *J. Phys. Chem.* **1990**, *94*, 8897–8909.
(52) Rappé, A. K.; Casewit, C. J.; Colwell, K. S.; Goddard, W. A., III.; Skid, W. M. *J. Am. Chem. Soc.* **1992**, *114*, 10024–10035.
(53) Zhao, Y.; Truhlar, D. G. *J. Chem. Theory Comput.* **2005**, *1*, 415–432.
(54) Cammi, R.; Mennucci, B.; Tomasi, J. *J. Phys. Chem. A* **2000**, *104*, 5631–5637.
(55) Cammi, R.; Mennucci, B.; Tomasi, J. *J. Phys. Chem. A* **1999**, *103*, 9100–9108.
(56) Cossi, M.; Rega, N.; Scalmani, M.; Barone, V. *J. Chem. Phys.* **2001**, *114*, 5691–5701.
(57) Cossi, M.; Scalmani, G.; Rega, N.; Barone, V. *J. Chem. Phys.* **2002**, *117*, 43–54.
(58) Cossi, M.; Scalmani, G.; Rega, N.; Barone, V. *J. Comput. Chem.* **2003**, *24*, 669–681.
(59) Barone, V.; Cossi, M.; Tomassi, J. *J. Chem. Phys.* **1997**, *107*, 3210–3221.

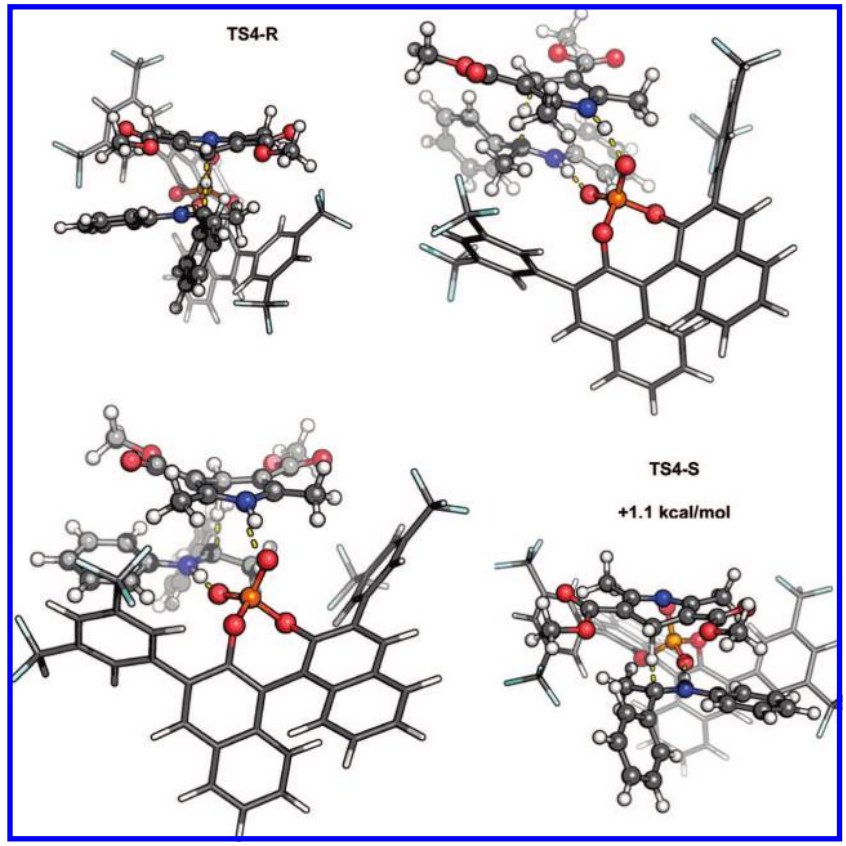

Figure 6. Transition states found for the Rueping-catalyzed reaction.

In order to understand the origin of the enantioselectivities obtained with the catalysts, steric interactions were estimated. Starting from the geometries optimized for transition structures, ONIOM single-point evaluations were performed using MPWB1K/6-31G** for the high-level layer and UFF method for the low-level layer. The energy obtained for the high-level layer does not include the contributions from the steric interactions between transition structure and bulky groups in the catalyst. These values were subtracted from the gas phase energy obtained in single-point evaluation of the full structure using MPWB1K/6-31G** level of theory in the previous calculation (free solvation energies were not used to avoid contribution from the cavity in PCM models). Comparison of the values obtained for every transition structure to the values offered by the most stable transition structure gave an estimate of the relative steric interactions.

Results and Discussion

An exhaustive survey of the reaction of the hydride donor with a phosphate−imine complex yielded four transition states corresponding to Mechanism B, of which two correspond to the *E* conformation and two to the *Z* conformation of the imine. The lowest-energy transition structures of each set (TS1-Z, TS1-E) are illustrated in Figure 3, and details of the rest are available in the Supporting Information. Twelve transition states were found for Mechanism A, with six each proceeding from *E* -and *Z*-imine conformations (The two lowest-energy transition states are shown as TS2-Z, TS2-E in Figure 3). These have activation barriers more than 10 kcal/mol higher than those of the transition structures corresponding to Mechanism B. Two additional transition structures have been found (TS3-Z, TS3-E), in which the imine group is protonated and the phosphate catalyst establishes a single interaction with the NH of the Hantzsch ester. We label this Mechanism C. Like Mechanism A, it has a higher energy barrier than Mechanism B.

The transition structures in which the imine has a *Z* conformation (TS1-Z, TS2-Z, TS3-Z) are more stable than those in which the *E* conformation is present, although calculations with the same level of theory shows that that the *E*-imine ground state is more stable by 2.9 kcal/mol. A fast *E*/*Z* equilibrium in the imines can be expected under the reaction conditions since the formation of the imine is fast (the imines can be generated *in situ*[8,11,14,60]), so the reaction should proceed through the *Z* transition state. This is important in understanding enantioselectivities, because hydride addition on the same face will yield opposite enantiomers for *Z* and *E* conformations. The geometries of both transition structures and starting materials show that the benzyl ring twists in the *Z* conformers, in order to avoid steric interactions between the two aromatic rings (Figure 4). This may reduce resonance stabilization (torsional angles: *Z*-imine: 46°; *E*-imine: 5°; TS1-Z: 43°; TS1-E: 16°). We have quantified the extent of this effect using second-order perturbation theory analysis on the basis of the NBOs. Our results show an additional resonance stabilization of 10.4 kcal/mol for the *E*-imine, but only 2.9 kcal/mol in the *E* transition structure. This is expected since the reaction reduces the imine C−N double bond character as it proceeds. Other destabilizing effects for the *E* conformation, including higher steric interactions between phenyl and methyl groups in the imine and the transition structures, reduce the overall stabilization of the *E*-imine to only 2.9 kcal/mol, and make the *Z* transition structure 2.5 kcal/mol more stable.

The Rueping model for the stereoselectivity of the reaction, based on the crystal structure of a chiral Brønsted acid, uses the *Z* conformation of the imine.[7] This counterintuitive choice

(60) Vachal, P.; Jacobsen, E. N. *J. Am. Chem. Soc.* **2002**, *124*, 10012–10014.

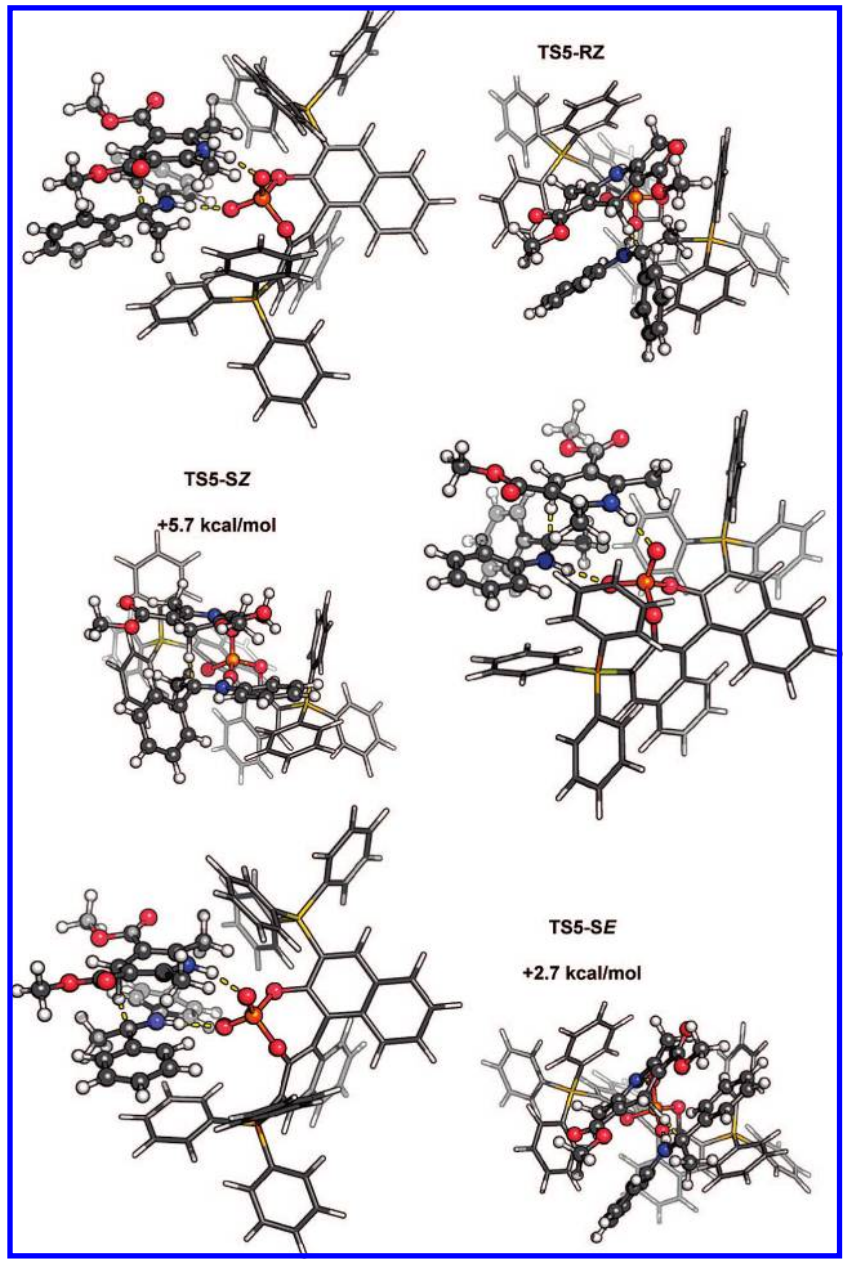

Figure 7. Transition states found for the MacMillan-catalyzed reaction.

gives the stereochemical result observed in the experiments. Our calculations demonstrate that the *Z* conformer is on the lowest-energy route to the product, and so is the best choice for the model. The calculations also fit the results for the cyclic substrates that have been reported.[9,11]

The achiral model catalyst does not offer an explanation for the asymmetric induction, since it lacks the bulky substituents present in chiral catalysts. We have, therefore, performed hybrid QM/MM ONIOM calculations. The Rueping[7] catalyst (R_3 = 3,5-(CF_3)-phenyl in Scheme 1, 72% ee) and MacMillan[11] catalyst (R_3 = Ph_3Si, 93% ee) were chosen for these studies (Figure 5) as the different enantioselectivities observed in these reactions make it possible to test the validity of the proposed mechanism: quantum chemical calculations should not only predict the absolute configuration of the major enantiomer but also the degree of selectivity observed.

As in previous studies, transition structures showing both *Z*- and *E*-imine conformations have been found. For the Rueping catalyst, higher-energy differences in favor of *Z* transition states are observed, probably due to steric interactions between bulky groups in the catalyst and imine aromatic rings in the *E* conformation (TS4-S*E*, +9.4 kcal/mol; TS4-R*E*, +6.5 kcal/mol, see Supporting Information). In the unfavorable *Z* transition structure (TS4-S, Figure 6), this catalyst places the 3,5-(CF_3)-phenyl group near the *N*-phenyl group in the imine. The zero-point energy of this structure is 1.1 kcal/mol higher than that for the most stable transition state (TS4-R, Figure 6), in excellent agreement with experimental results. A comparison of the steric interactions of these two transition state structures indicates a destabilization of 1.9 kcal/mol for this structure.

For the MacMillan catalyst, two *Z* and two *E* diastereomeric transition structures have also been located. Like the previous catalyst, the most stable structure corresponds to a *Z* transition structure in which the bulky triphenylsilyl groups avoid interactions with *N*-phenyl group in the imine. In the diastereomeric *Z* transition structure (Figure 7, TS5-SZ), these interactions are

Table 1. Stereochemistry[a] of Majority Product of Different *R*-BINOL-Phosphoric Acid-Catalyzed Reaction of Aryl Imines

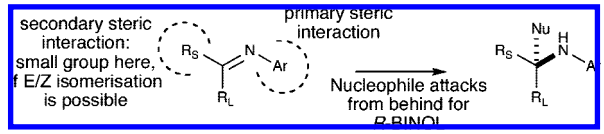

Entry	Nucleophile	Imine	Product	Reference
1		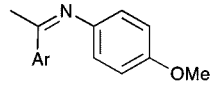	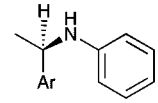	70 - 84% e.e.[7] 83 - 95% e.e.[11] 90 - 93% e.e.[15]
2		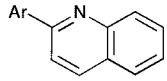	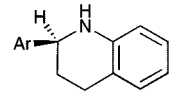	87 - >99% e.e.[9]
3		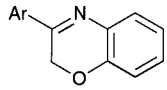	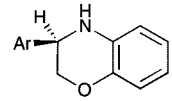	93 - >99% e.e.[10]
4	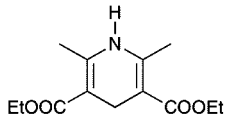	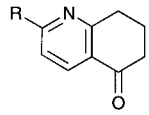	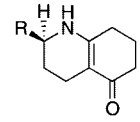	87 – 92% e.e.[16]
5		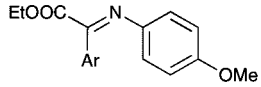	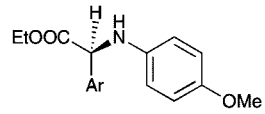	95 - 98% e.e.[13]
6		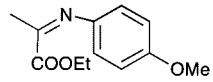	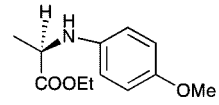	99% e.e.[13]
7		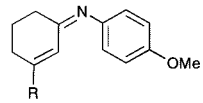	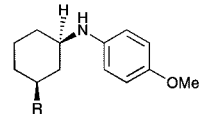	83 - 96 e.e. d.r.: 2:1 to 99:1[14]
8	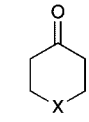	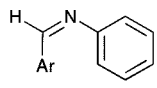	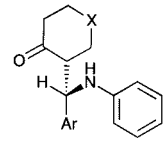	75 – 98% e.e. d.r.: 77:23 to 98:2[21]
9			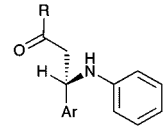	80 - 86 % e.e.[21]
10	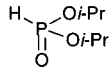	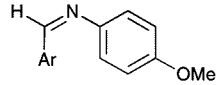	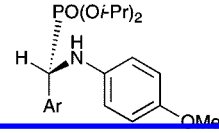	52 - 90 % e.e.[35]

[a] Stereochemistry shown for product obtained by (*R*)-BINOL-phosphoric acid catalyst.

so important that this structure is destabilized by 5.7 kcal/mol. The steric interactions destabilize the structure by 3.2 kcal/mol with respect to the TS5-R structure. The formation of the S product is more favorable from the *E* transition state (Figure 7, TS5-S*E*), which has a zero-point energy 2.7 kcal/mol higher than that of the TS5-R structure, in good agreement with experimental results. In this structure, the catalyst places a phenyl ring of the triphenylsilyl group parallel to the benzyl ring in the substrate, avoiding steric interactions. This is confirmed by a small (0.1 kcal/mol) steric interaction energy difference in favor of this structure with respect to TS5-R. Although this transition state is free of steric interactions, the preference for the *Z* transition state explains the enantioselectivity of the reaction, just as it did for the smaller model catalyst. The *E* transition state corresponding to the *R* enantiomer is destabilized by 8.6 kcal/mol (see Supporting Information).

These calculated energy differences can be used to calculate the enantiomeric excesses that should be expected in these reactions, at the temperatures at which they were performed. The Rueping catalyst is reported as producing 72% ee at 60 °C.

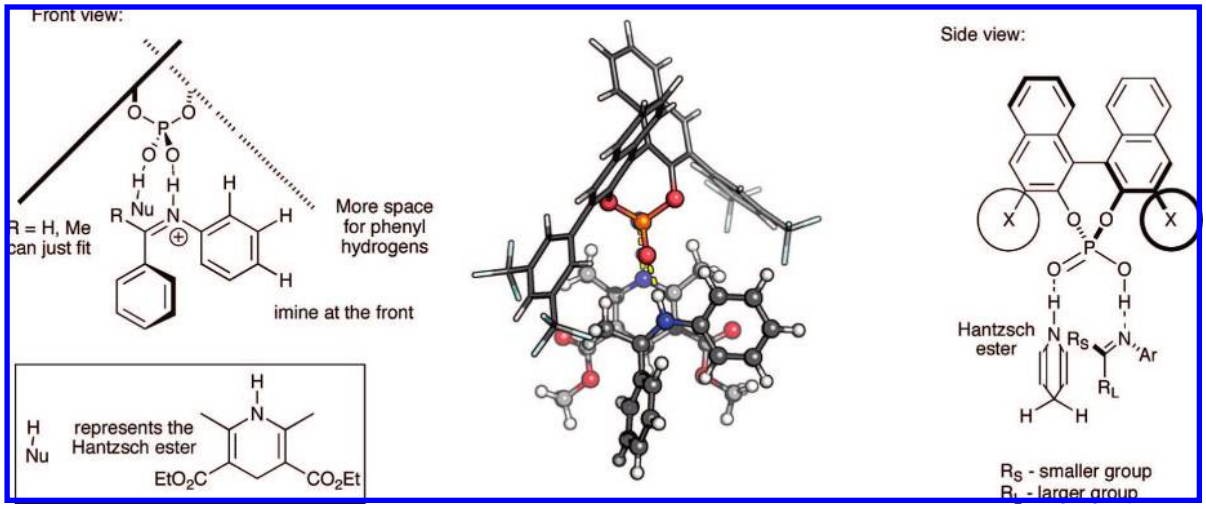

Figure 8. Model proposed for predicting the stereochemistry of BINOL-phosphoric acid-catalyzed Hantzsch ester imine reduction.

The calculation suggests a value of 70% ee for this temperature. The MacMillan catalyst gives 93% ee at 40−50 °C. The calculation suggests a value of 97% ee at 45 °C. Both of these calculated values are close to the experimental ones, and the relative efficacy of the two catalysts is reproduced very well.

On the basis of these studies, we propose a simple model to predict the stereochemistry of the major product of this reaction (Figure 8). This model considers three interactions between the catalyst and the transition state structure: the phenylimine, in *Z* conformation if possible, is complexed to the catalyst (first point interaction) leaving the more sterical demanding groups (usually the *N*-phenyl or PMP group and the largest substituent of the imine) toward the less hindered sites of the catalyst (second point interaction); the Hantzsch ester is then complexed to the other phosphoric acid oxygen of the catalyst (third point interaction), and hydride transfer takes place from this face. This model predicts the right stereochemistry for the acyclic aryl imines[7,11,14] (Table 1, entry **1**). For reduction of cyclic substrates (Table 1, entries 2−4), the substrate is not able to change the *E*−*Z* conformation in order to accommodate the largest group outside the catalyst. The stereochemistry of the reaction is consistent with the imine nitrogen aromatic ring placed in the less hindered side of the catalysts, irrespective of the size of the α-substituent. A reasonable explanation is that this carbon is pyramidal in the transition state (unlike the nitrogen atom), allowing the large substituent to avoid steric interaction with the catalyst. This agrees with the results that we have obtained for *E* imine transition states, showing a lower energy when the *N*-phenyl group is placed away from the bulky catalyst groups.

For the reaction of α-imino esters (entries **5** and **6**) the stereochemistry depends on the relative size of the other substituent. In the case of large substituents, such as aromatic rings (entry **5**), the more stable transition state exposes the ester group toward the catalyst. For the smaller methyl substituent (entry **6**), the conformation of the imine changes, yielding the opposite enantiomer. The model can also be applied to a cascade 1-4 and 1-2 reduction (entry **7**), correctly explaining the stereochemistry of both 1,4- and 1,2-hydrogenations. The right stereochemistry is also predicted for other nucleophiles, such as enols in a Mannich addition (entries **8** and **9**) and phosphites (entry **10**).

Conclusions

Calculations on the reaction mechanism show that Mechanism B is much more effective than Mechanism A in explaining the experimentally determined enantioselectivities. A preference for *Z* imine transition states is observed, which is important to the stereochemical course of the reaction. The different catalysts determine the stereochemistry of the products using similar steric interactions. Mechanism B allows us to interpret the enantioselectivity according to the "three-point contact model":[37] two H bonds with the phosphate and the effect of steric hindrance. A qualitative model to predict the stereochemistry of the reaction is proposed. In order to get quantitative results, the effect of the E transition states which provide an important minor pathway in some cases (for example, in the case of MacMillan catalyst), must also be considered.

Acknowledgment. This research was supported by a Marie Curie Intra-European Fellowship within the 6th European Community Framework Programme MEIF-CT2006-040554. We acknowledge the use of CamGrid service in carrying out this work, and Dr. Charlotte Bolton for the IT support.

Supporting Information Available: Description of the computational methods; complete reference 47; Cartesian coordinates of optimized structures. This material is available free of charge via the Internet at http://pubs.acs.org.

JA800793T